



The Performance of the LHCb Muon Identification Procedure

E. Polcarpo, M. Gandelman

Instituto de Física — Universidade Federal do Rio de Janeiro - UFRJ

Abstract

This note describes the LHCb offline muon identification procedure and the algorithm parameters tuning using a Monte Carlo sample of $B \rightarrow J\psi K_s$ events. The performance is also presented for a sample of $b\bar{b}$ inclusive events.

Work partially supported by CNPq, FAPERJ, FINEP, Fundação Universitária José Bonifácio (FUJB) and by ALFA-EC funds in the framework of Program HELEN (High Energy Physics Latinoamerican-European Network).

Contents

1	Introduction	2
2	Offline muon identification algorithm	3
3	Parameters tuning	4
3.1	FOI parameters	4
3.1.1	Effect of including M1 on the IsMuon requirement	6
3.2	Tuning of likelihoods	6
4	Performance	7
4.1	Muon Track Matching	7
4.1.1	Sources of Misidentification	9
4.2	Difference of Log-Likelihoods criterium	9
4.3	Combined DLL Criterium	11
4.4	Rejection of Tracks Sharing Hits	13
5	Conclusions	14

1 Introduction

The LHCb Muon System [1], shown in Figure 1, is composed of five stations (M1-M5) of rectangular shape, placed along the beam axis. Stations M2 to M5 are placed downstream of the calorimeters and are interleaved with iron absorbers 80 cm thick to select penetrating muons. The minimum momentum required of a muon to cross the five stations is approximately 6 GeV/c since the total absorber thickness, including the calorimeters, is approximately 20 interaction lengths. Station M1 is placed in front of the calorimeters.

The inner and outer angular acceptances of the muon system are 20 (16) mrad and 306 (258) mrad in the bending (non-bending) plane respectively. Given the large particle flux variation in passing from the central part, close to the beam axis, to the detector border, each station is subdivided into four regions with different pad dimensions (Figure 2). Region and pad sizes scale by a factor two from one region to the next. The transverse dimensions of the five stations scale with the distance from the interaction point.

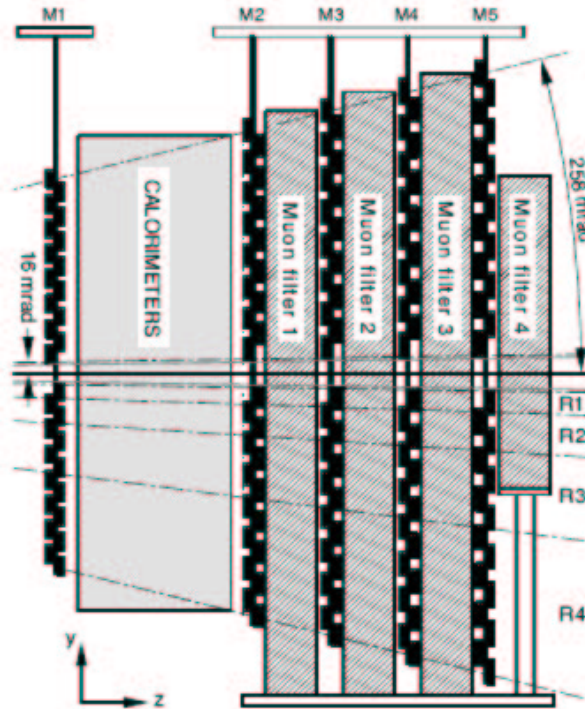


Figure 1: Side view of the LHCb Muon System in the y, z plane.

The basic idea of the offline muon identification algorithm is to look for hits around the track extrapolation in a window which is called *Field of Interest* (FOI). As the algorithm depends on the tuning of the FOI as a function of momentum one can expect that the inclusion of a more detailed description of the detector in the simulation implies a new tuning.

The so called *Computing Data Challenge 2006* (DC06) was an exercise to the LHCb computing model and at the same time produced samples for the analyses which will be presented in the forthcoming Physics Book. Compared to the performance presented in [6], the muon efficiency obtained with the DC06 data was shown to be reduced when the FOI optimized with the samples available for the study presented in [6] were used. The observed reduction was mainly due to the inclusion of a new description of the beam pipe and supports geometry in the

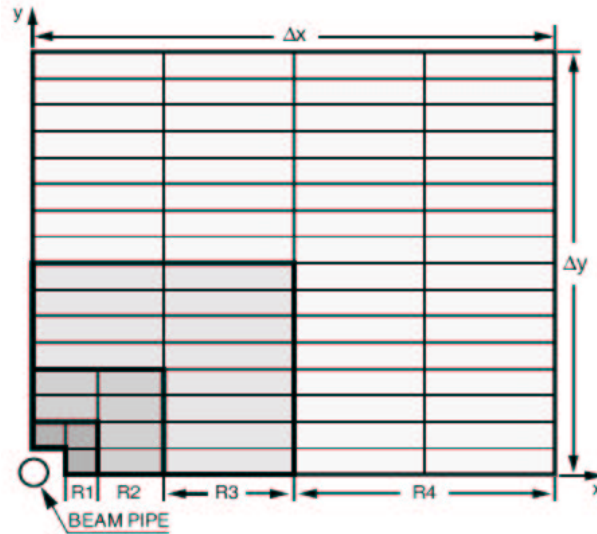


Figure 2: Front view of one quadrant of muon station 2, showing the dimensions of the regions.

simulation, according to the actual installation in the experiment site, as well as of new values of the crosstalk probabilities for the Muon system detectors.

The cross-talk probabilities have been reduced for almost all chamber types, according to test beam results. Compared to the values used in [6], there were reductions ranging from 30% to 60% in the y direction of stations M2 and M3 and from 40% to 70% in the x direction of the same stations [7]. The FOI sizes that should be essentially given by MCS and granularity were artificially reduced due to an excess of crosstalk hits. Having to increase the FOI sizes we must expect an increase on the misidentification rate due to the higher probability to find a hit within them.

To tune the FOI parameters for the DC06 samples, we have used about 350k $B \rightarrow J/\Psi(\mu^+\mu^-)K_s$ events¹.

2 Offline muon identification algorithm

In order to be selected as a Muon, a track reconstructed in the spectrometer must be matched to hits in a number of Muon Stations which depends on momentum according to Table 2. A hit is considered to match a track if it is within a field of interest around a linear extrapolation of the track direction in M1 to the corresponding station. The size of the FOI is given essentially by MCS and therefore varies with the track momentum, except in M1, which is located before the calorimeter. Since the different regions of the Muon system have different detector granularities and correspond to different paths in the detector material, the size of the FOI is tuned separately for each of the 4 regions of the Muon system, in all the 5 stations.

For each track, two likelihoods are computed using only the information from the Tracking and Muon systems: one for the muon and another one for the non-muon hypothesis. The distribution of the average of the squared distance between the extrapolation point and the fired pads within the FOI of the stations required to have hits ($|Dist|^2$) is used to build these likelihoods.

¹Produced with **Gauss v24r3** [2], digitized with **Boole v11r2** [3] and reconstructed with **Brunel v30r10** [4]

A sample of tracks matching a muon from the MC truth table is used for the muon hypothesis and a sample of tracks that do not match a MC particle from the truth table which is not a muon and do not decay into a muon within the detector is used for the non-muon hypothesis.

Another variable that can be used to discriminate between muons and non-muons, called from here on *NShared*, is the number of additional tracks in the event which share hits with this track and have a smaller $|Dist|^2$. It is built to reduce the contamination due to non-muons which point in the same direction of muons from the same event. This kind of contamination increases with the number of muons in the event. Although *NShared* was shown to be useful to increase the purity of muons selected for flavour tagging [8], it was not included in the likelihood computation because it reduces the muon selection efficiency more than the selections of some decay channels may need.

Track momentum (GeV/c)	Required stations
$3 < p < 6$	M2+M3
$6 < p < 10$	M2+M3+(M4 or M5)
$p > 10$	M2+M3+M4+M5)

Table 1: Stations required to have a hit within FOI for tracks at different momentum ranges.

It is important to note that only the so called "preselected" tracks are passed through the muon identification algorithm. Preselected tracks have momentum greater than 3 GeV/c and point into the Muon System (station M3). About 50% of the muons with $p = 3$ GeV/c reach M3 [9].

Requiring the matching is the most efficient way to select a muon. To further reduce the contamination, one can use a cut on the difference between the logarithm of likelihoods for the muon and background hypotheses (DLL). This difference can be added to the log-likelihood differences provided by other sub-systems, as the RICH and Calorimeters, to achieve a better discrimination. The combined difference of log-likelihoods (CDLL) is better described in [10]. Another possibility is to cut on *NShared*. In Section 4 the performance of these selection criteria is analyzed.

3 Parameters tuning

The parameters of the algorithm which must be tuned are the sizes of the FOI and the likelihoods for the two opposite particle hypotheses. For now, all the parameters are taken from the simulation. Strategies to obtain these parameters using data are under study [12].

3.1 FOI parameters

The size of the elliptic FOI around the track extrapolation point in each region of each station is given by the momentum dependent functions

$$p0_{x,y} + p1_{x,y} * exp(-p2_{x,y} * p), \quad (1)$$

where x and y denote the two directions of the plane transverse to the beam in the bending and non-bending planes, respectively. The parameters of this function are tuned to maximize the efficiency over the full momentum range with misidentification rates on the percent level.

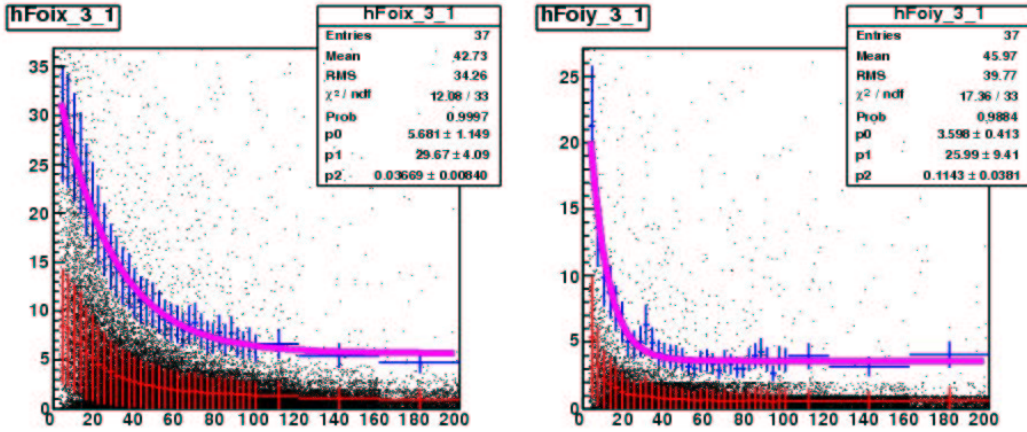


Figure 3: Distributions of the mean distance from extrapolation to closest pad hit, in half pad units, versus muon momentum. The red markers correspond to the profile histogram, showing the mean distance and the RMS as error bar for each momentum interval. The magenta lines are fits to the curves $(h\text{Foix}, y + 3.5 \cdot \text{RMS})$ in the x (left plot) and y (right plot) directions.

N	Total Efficiency (%)	Total Misid Rate (%)
2	89.17 ± 0.09	2.12 ± 0.01
3	95.62 ± 0.06	3.17 ± 0.01
3.5	96.65 ± 0.05	3.78 ± 0.01
4.	97.22 ± 0.05	4.45 ± 0.01

Table 2: Total efficiency and misidentification rate, for N going from 2 to 4.

In order to make this tuning, we plot the 2-dimensional distribution of the distance from track extrapolation to the closest pad hit, in half pad units, versus momentum, for a sample of muons matching the MC truth table, and the corresponding profiles, for the x and y directions. From the profile plots, we get the mean distance ($h\text{Foix}$ and $h\text{Foiy}$) and the RMS for the different momentum bins. An example plot can be seen in Fig. 3, for the inner region of the third station.

The functions given in Eq. 1 are then fitted to the profile histograms obtained with the mean value added to a number N of RMS varying from 2 to 4. The fit parameters for different values of N are used to compute $IsMuon$. The efficiency and the misidentification rate as a function of momentum are shown in the left and right plot of Figure 4. Efficiency is defined as the ratio between the number of true muons with $IsMuon = 1$ and the number of true muons preselected. The misidentification rate has an analogue definition for tracks in the background sample.

As expected, when N increases both the efficiency and the misidentification rate increase. The efficiency is equivalent for the one obtained with DC04 data for $N = 3.5$ and $N = 4$. Table 2 shows the total efficiency and misidentification rate (integrated over the full momentum range) for the same N values. While the total efficiencies for $N = 3.5$ and $N = 4$ are equivalent, the total misidentification rate is reduced when we use $N = 3.5$. We then choose the FOI parameters for $N = 3.5$ as the default muon identification FOI parameters for DC06.

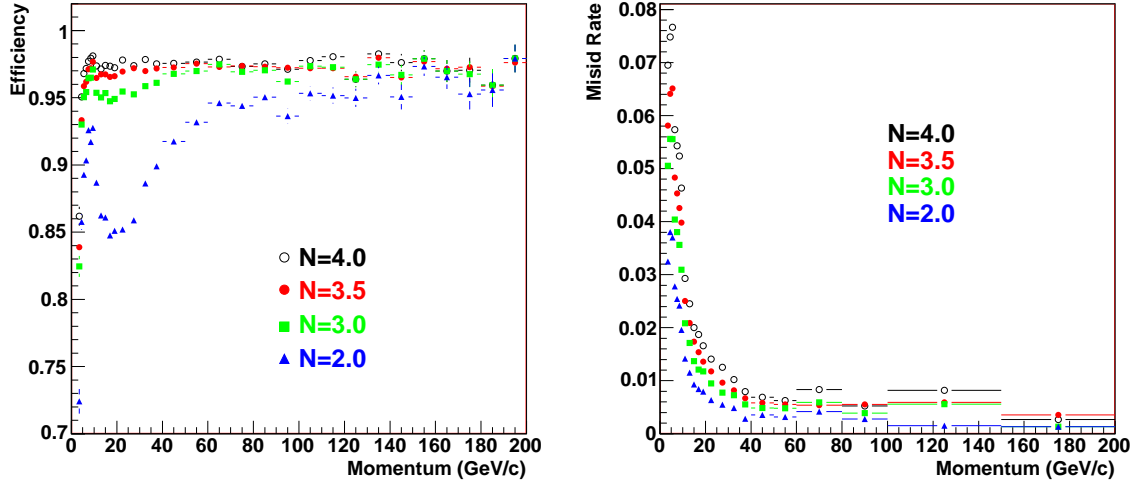


Figure 4: The efficiency for identifying muons (left) and the misidentification rate (right) as a function of momentum, for N going from 2 to 4.

3.1.1 Effect of including M1 on the IsMuon requirement

The use of the hits in the muon station 1 (M1) was studied. We used the FOI parameters determined with 3.5 RMS added to the mean value of the distance from hit to track extrapolation in the x and y directions and required, in addition, at least one hit in station M1, within a FOI of increasing size around the track position in M1. As seen from Table 3.1.1, no improvement in the overall performance is obtained. For that reason, it was decided not to use M1.

M1 Foi (pad length)	Efficiency (%)	Total Misid Rate (%)
3	95.88 ± 0.05	3.72 ± 0.01
4	96.11 ± 0.05	3.75 ± 0.01
5	96.30 ± 0.05	3.76 ± 0.01
6	96.43 ± 0.05	3.77 ± 0.01
7	96.53 ± 0.05	3.77 ± 0.01
no	96.65 ± 0.05	3.78 ± 0.01

Table 3: Efficiency and total misidentification rates when using M1 hits to build the IsMuon requirement

3.2 Tuning of likelihoods

To obtain the distribution used to build the likelihoods for muons and for the background, the average of the squared distance between the track extrapolation to a given muon station and the hits inside the FOI is computed. This squared distance is then plotted for true muons and for non-muon tracks. The distributions are fitted with a combination of 3 Landau functions.

In Figure 5, the distribution of the squared distance and the result of the fit are superimposed.

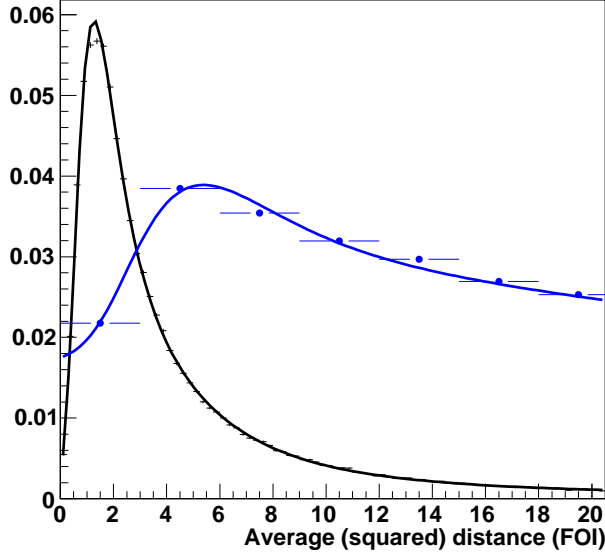


Figure 5: Average squared distance from track extrapolation to hits inside the FOI. Black crosses and curve represent the muons while the blue points and function, the non-muon tracks.

Once the Landau parameters are determined, the likelihoods can be computed for any given track using the squared distance of this track. The difference between the log of the likelihoods for the muon and non-muon hypotheses (DLL) can be used as a discriminating variable.

4 Performance

The performance of the identification algorithm and the remaining contamination was evaluated with 100k $B \rightarrow J/\Psi K_s$ and $b\bar{b}$ inclusive events, using Boole v12r6 and Brunel v30r10.

4.1 Muon Track Matching

The global performance obtained by just requiring the Muon System matching (IsMuon=1) is shown in Table 4, where the efficiency (ϵ_μ) and misidentification rate (\mathcal{R}) are integrated over the whole momentum spectrum. Figure 6(a) shows the performance as a function of momentum. Open symbols correspond to the results obtained with the $B \rightarrow J/\Psi K_s$ sample while the solid markers refer to the $b\bar{b}$ inclusive sample. The efficiency curve reaches the 95% level around 5 GeV/c and its shape is independent of the sample. This can be better visualized in Fig. 6(b), which shows an amplified view of the low momentum part of the same plot. The $b\bar{b}$ sample presents a lower total efficiency because it is more populated with low momentum tracks. The misidentification rate has a big contribution from decays in flight (considered as a contamination for the identification algorithm), which is shown separately. The higher number of muons in the $B \rightarrow J/\Psi K_s$ events is responsible for the higher value of \mathcal{R} measured.

Figure 7 shows the behaviour of ϵ_μ e \mathcal{R} as a function of the polar angle. The increase of misidentification rate with polar angle is due to the correlation between momentum and transverse momentum which makes low momentum tracks to have higher polar angle. The

sample	ϵ_μ	\mathcal{R}
$B \rightarrow J/\Psi K_s$	96.44 ± 0.04	4.05 ± 0.01
$b\bar{b}$	95.32 ± 0.16	3.44 ± 0.01

Table 4: The total efficiency ϵ_μ for identifying muons and the total misidentification rate \mathcal{R} measured in two different samples.

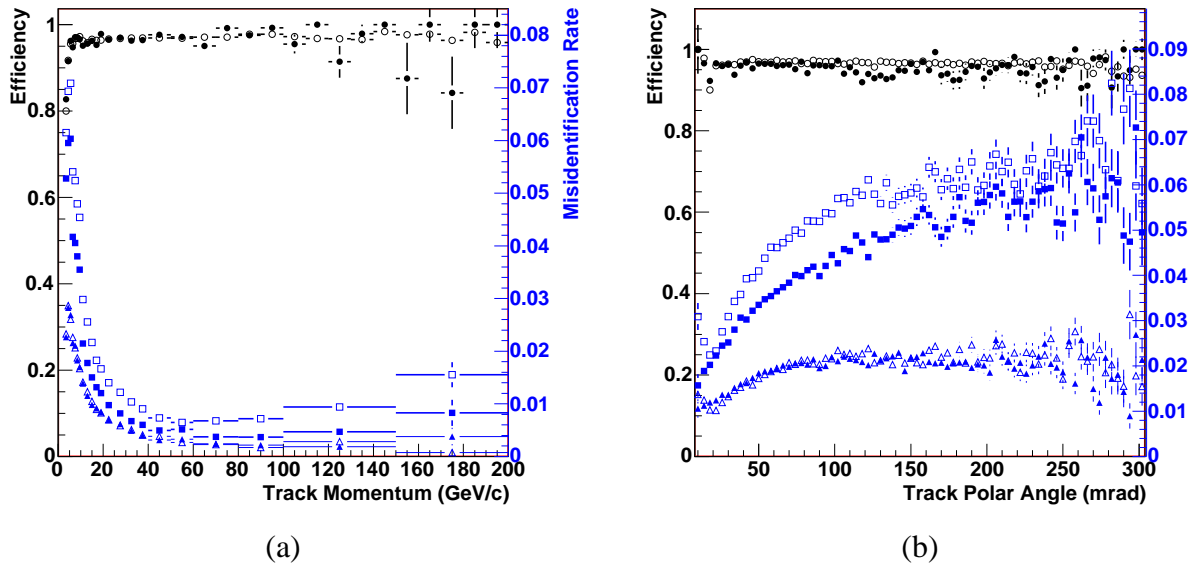


Figure 6: The efficiency for identifying muons (circles) and the total misidentification rate (squares) as a function of the momentum (a). The contribution of muons from the decays in flight is shown separately by the triangles. Open and filled markers correspond to the curves obtained using a sample of $B \rightarrow J/\Psi K_s$ and $b\bar{b}$ events, respectively. An amplification of the low momentum part is also shown (b).

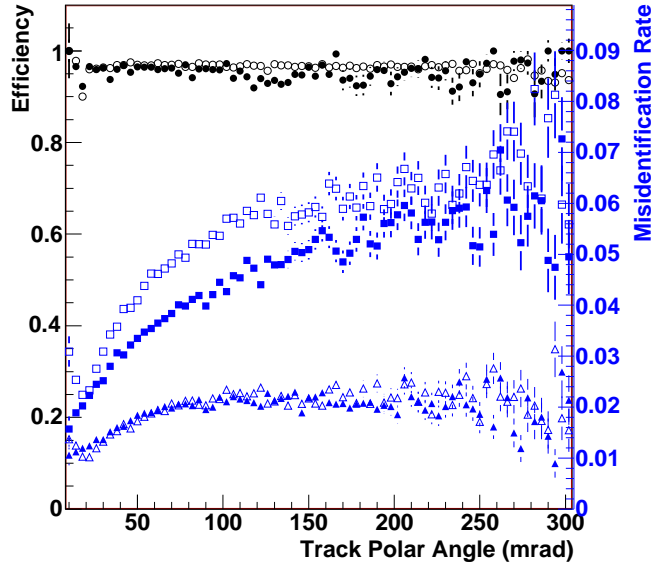


Figure 7: The efficiency for identifying muons (circles) and the total misidentification rate (squares) as a function of the polar angle. The contribution of muons from the decays in flight is shown separately by the triangles. Open and filled markers correspond to the curves obtained using a sample of $B \rightarrow J/\Psi K_s$ and $b\bar{b}$ events, respectively.

sizes of the FOI also increase with polar angle, due to MCS and detector granularity, making the probability to find a random hit within FOI increase accordingly.

4.1.1 Sources of Misidentification

The sources of misidentification were studied and we concluded that around 71% of it is due to real muons either from decays or from a nearby muon from the origin or from decays in flight of other nearby particles. Around 22% is due to random combinations, while the remaining 7% could be due to a calorimeter shower leaking to the muon system.

The breakdown of the different contributions for $B \rightarrow J/\Psi K_s$ and $b\bar{b}$ inclusive events is shown in Table 5.

4.2 Difference of Log-Likelihoods criterium

The difference of the log-likelihoods (DLL) calculated for the muon and non-muon hypotheses is used as a discriminating variable. In Figure 8, the DLL is shown for muons and non-muon tracks matching hits in the Muon System and selected in the $B \rightarrow J/\Psi K_s$ and $b\bar{b}$ inclusive samples. The solid area shows the contribution from the decays in flight separately. The different behaviour of the DLL distributions is related to the different momentum spectrum of the tracks in the different data samples.

The effect of changing the DLL cut is shown in the plots of Figure 9 where one can see that the IsMuon efficiency is recovered for cuts lower than -4. An efficiency of $(90.17 \pm 0.07)\%$ is obtained for a misidentification rate of $(1.41 \pm 0.01)\%$ in the $B \rightarrow J/\Psi K_s$ sample, when

	J/Psi Ks	bbincl
Total Misid	4.05 %	3.44 %
Due to decays	1.66 %	1.72 %
Due to muon hits in at least 66% of the stations (2/3,3/4,2/2,3/3,4/4)	1.22 %	0.73%
Divided in :		
Muons originated before the calorimeter	1.17 %	0.67 %
Muons originated in the calorimeter	0.05 %	0.06 %
Due to Random Combinations	1.17%	0.99 %
Divided in :		
No MC association in at least 66% of the stations (2/3,3/4,2/2,3/3,4/4)	0.83 %	0.75 %
Random combinations of hits	0.34 %	0.24 %

Table 5: Sources of misidentification for $B \rightarrow J/\Psi K_s$ and $b\bar{b}$ inclusive events.

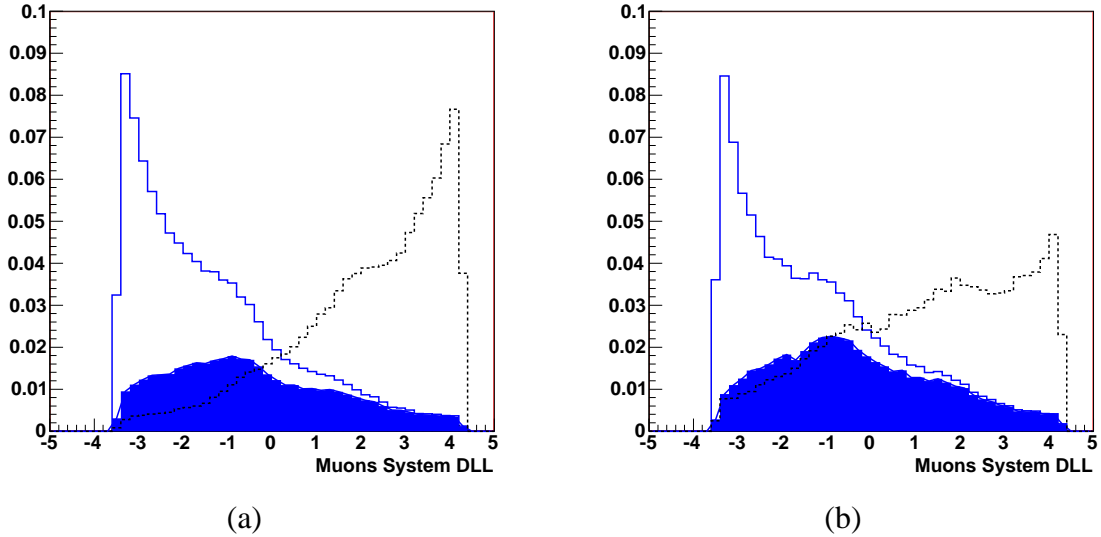


Figure 8: DLL for muon (full line) and non-muon tracks (dashed line) in the $B \rightarrow J/\Psi K_s$ (a) and $b\bar{b}$ inclusive (b) samples. The solid area shows the decays in flight separately.

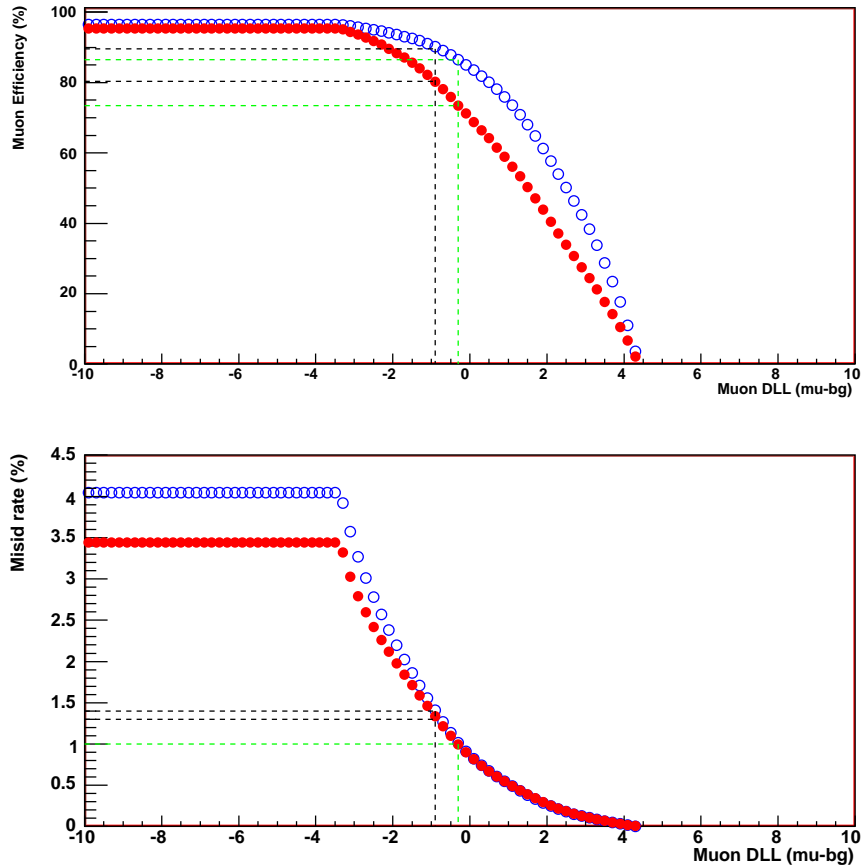


Figure 9: Muon efficiency (top) and misidentification rate (bottom) as a function of the DLL cut. The open circles show the performance for $B \rightarrow J/\Psi K_s$ and the solid ones, for $b\bar{b}$ inclusive events. The lines represent the cut that gives 90% efficiency and the one which puts the contamination down to 1% in the $B \rightarrow J/\Psi K_s$ inclusive sample.

the cut $DLL > -1.0$ is applied. Figure 10 shows the performance as a function of momentum when this cut is applied. To reduce the misidentification rate down to 1% using only the Muon System DLL, a cut on $DLL > -0.4$ must be applied, diminishing the efficiency to approximately 86%. In the $b\bar{b}$ events, an efficiency of 73% is observed for the same DLL cut, with a similar misidentification rate.

4.3 Combined DLL Criterion

The DLL obtained using only the muon system can be further improved by combining it with the DLL provided by other LHCb sub-systems. This is better seen in the plot of Figure 11. In this Figure, the two top curves (blue and pink) were obtained without using the muon system. The brown curve shows the muon system alone results and the final combination is represented by the lower curve, in black.

The effect of cutting on the combined DLL for $B \rightarrow J/\Psi K_s$ and $b\bar{b}$ inclusive events can be seen in the plots of Figure 12. For a cut on the combined DLL that keeps $(90.35 \pm 0.07)\%$ efficiency for identifying muons in the $B \rightarrow J/\Psi K_s$ events, the misidentification rate goes down

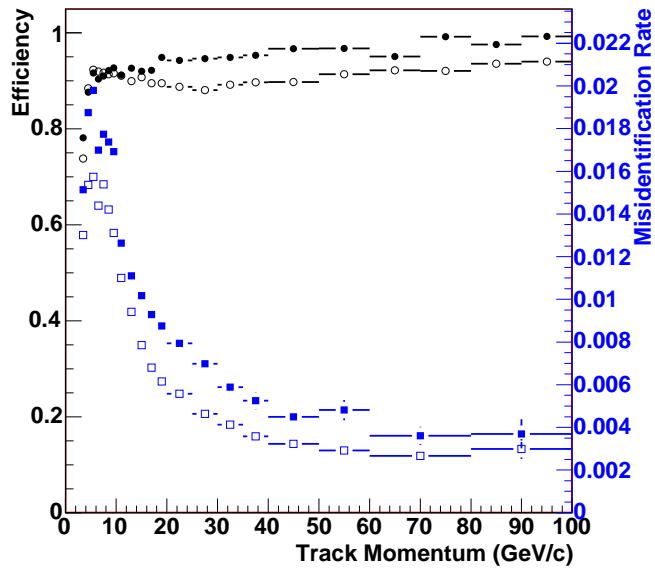


Figure 10: The efficiency for identifying muons and the misidentification rate as a function of the momentum. A cut of $DLL > -1$ was used to produce this plot. Open and filled markers correspond to the curves obtained using a sample of $B \rightarrow J/\Psi K_s$ and $b\bar{b}$ events, respectively.

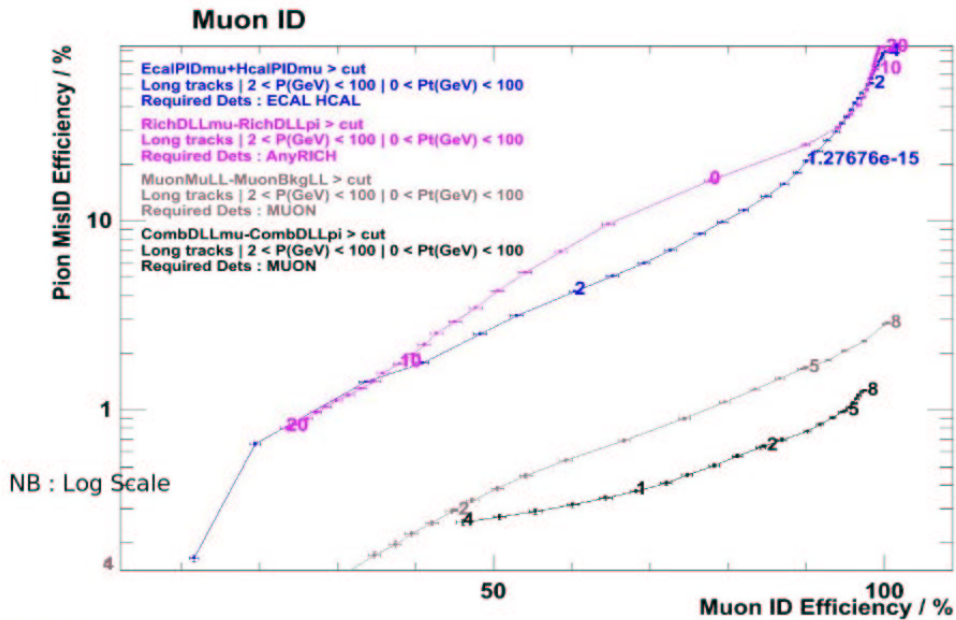


Figure 11: Misidentification rate versus efficiency for the various DLL combinations.

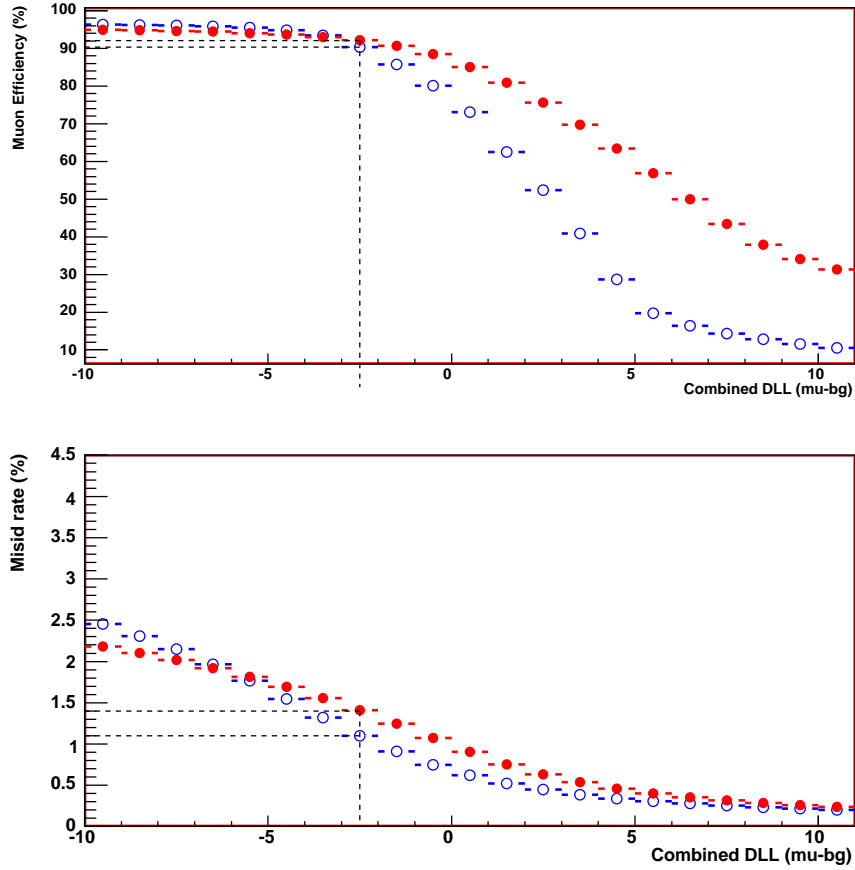


Figure 12: Muon efficiency (top) and misidentification rate (bottom) as a function of the DLL cut. The open circles show the performance for $B \rightarrow J/\Psi K_s$ and the solid ones, for $b\bar{b}$ inclusive events. The line represent the cut that gives 90% efficiency and 1.1% contamination.

to $(1.1 \pm 0.01)\%$, which can be compared to 1.4% for the DLL using only the Muon System. For the $b\bar{b}$ events, the same cut provides an efficiency of $(92.16 \pm 0.21)\%$ and a misidentification rate of $(1.41 \pm 0.01)\%$.

4.4 Rejection of Tracks Sharing Hits

To further reduce the misidentification rate, a cut on the number of tracks that share hits can be applied. The efficiency versus misidentification rate curve for $B \rightarrow J/\Psi K_s$ (open circles) and $b\bar{b}$ inclusive (filled circles) events is shown in Fig. 13. Figure 13(a) shows the performance after the matching requirement and Figure 13(b) after both the matching and the cut on the combined $DLL > -1$. Requiring that there is no other track in the event sharing hits ($N_{\text{Shared}} < 1$) is the hardest cut one can make. Table 4.4 shows the total efficiency and misidentification rate obtained for this cut when the two data samples studied are used. For the $B \rightarrow J/\Psi K_s$ sample, the misidentification rate is reduced by 53%, while the efficiency is reduced by 14%, when just the matching is required before $N_{\text{Shared}} < 1$. The $b\bar{b}$ sample presents a poorer performance, since the average number of muons per event is smaller: the efficiency is reduced by 7% for a misid rate reduction of 34%. In general, the results achieved with this cut used to

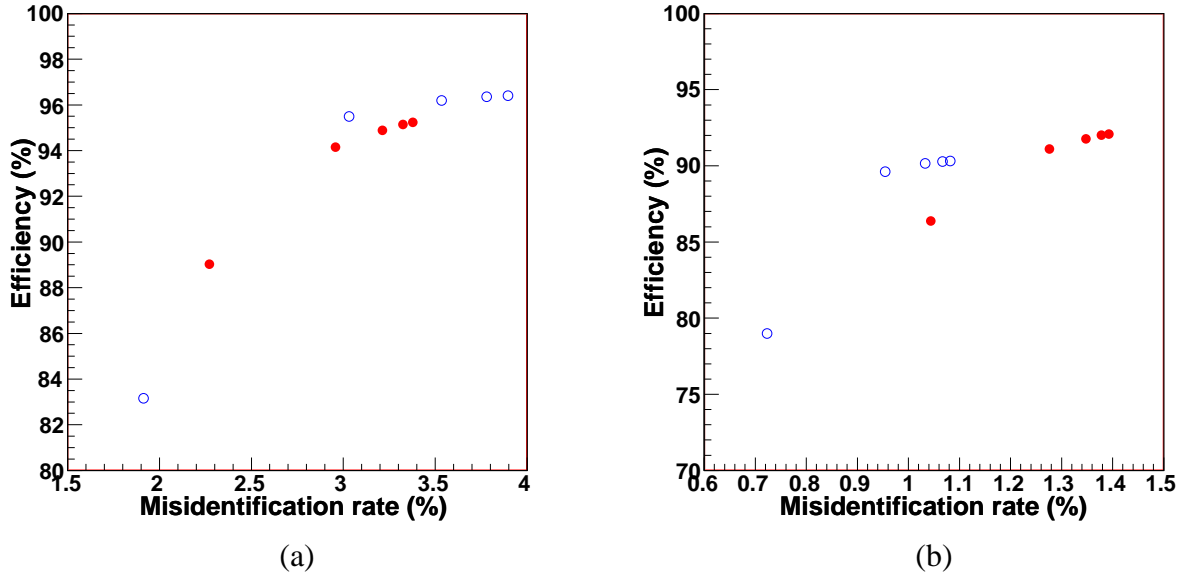


Figure 13: Muon efficiency versus misidentification rate for increasing cut values for NShared (NShared<1,2,3,4,5). Plot (a) shows the performance when the NShared cut is applied after the matching is required and (b) when both the matching and the cut on the combined DLL are required.

be better at the time of the Data Challenge in 2004. Better results obtained with a more recent version of the reconstruction software (Brunel v32r0), which has a tracking performance closer to the DC04 one, confirm that the tracking quality is very important to this criterium. Using this version, the efficiency and misidentification rate obtained by cutting on Nshared<1 after the IsMuon criterium are $(93.6\pm 0.8)\%$ and $(2.0\pm 0.1)\%$, respectively. While the efficiency is reduced by 2.8%, the misidentification rate is reduced by 50%, a quite important improvement. The numbers obtained for other cut values can be seen in Fig. 14.

Sample	IsMuon=1		IsMuon=1 and CDLL > -1	
	Efficiency (%)	Misid Rate (%)	Efficiency (%)	Misid Rate (%)
$B \rightarrow J/\Psi K_s$	83.16 ± 0.09	1.91 ± 0.01	79.00 ± 0.09	0.72 ± 0.01
$b\bar{b}$	89.03 ± 0.24	2.27 ± 0.01	86.37 ± 0.27	1.04 ± 0.01

Table 6: Performance of the cut NShared<1.

5 Conclusions

A new tuning of the offline muon identification software parameters was provided and the performance was shown for independent samples of $B \rightarrow J/\Psi K_s$ and $b\bar{b}$ inclusive events. An increase of the misidentification rate is observed with respect to previous studies [6] obtained with criteria that provide the same reference values for the total muon identification efficiency, due to basically two reasons. First, due to a real increase of the low energy background hit

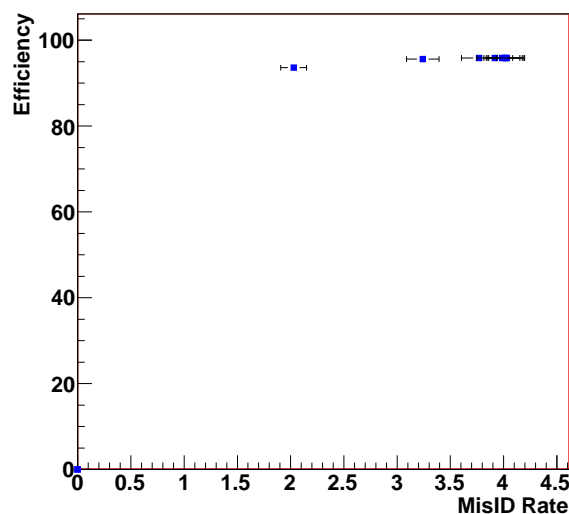


Figure 14: Muon efficiency versus misidentification rate for increasing cut values for NShared (NShared<1,2,3,4,5). The cut is applied after the matching is required in a sample of $B \rightarrow J/\Psi K_s$ events.

rate and of the FOI sizes, both increasing the probability to combine random hits in different stations. Finally, due to an underestimation of the pions and kaons decays in flight in reference [6]. In particular to the NShared discriminating criterium, preliminary studies are showing promising results with the most recent versions of the reconstruction software, which provide better tracking performance.

References

- [1] LHCb Collaboration, LHCb Muon System TDR, CERN-LHCC-2001-010, May 2001.
LHCb Collaboration, LHCb Muon System TDR Addendum 1, CERN-LHCC-2003-002, January 2003.
LHCb Collaboration, LHCb Muon System TDR Addendum 2, CERN-LHCC-2005-012, April 2005.
- [2] <http://lhcb-release-area.web.cern.ch/LHCb-release-area/DOC/gauss/>
- [3] <http://lhcb-release-area.web.cern.ch/LHCb-release-area/DOC/boole/>
- [4] <http://lhcb-release-area.web.cern.ch/LHCb-release-area/DOC/brunel/>
- [5] Needham, M., “Performance of the LHCb Track Reconstruction Software”, LHCb-2007-144.
- [6] Polycarpo, E.; Gandelman, M.; “Update on the Muon ID performance for the DC04 Monte Carlo data”, LHCb-2005-099; CERN-LHCb-2005-099.- Geneva : CERN, 23 Jan 2006.

- [7] Lanfranchi, G., “Update of chamber response parameters”, <http://indico.cern.ch/getFile.py/access?subContId=3&contribId=s1t0&resId=1&materialId=0&confId=a057281>
- [8] Calvi, M; Leroy, O; Musy, M, “Flavour Tagging Algorithms and Performances in LHCb”, CERN-LHCb-2007-058.
- [9] Polycarpo, E.; De Mello-Neto, J R T; “Muon identification in LHCb”, LHCb-2001-009, March 2001.
- [10] <https://twiki.cern.ch/twiki/bin/view/LHCb/GlobalParticleID>
- [11] <https://twiki.cern.ch/twiki/bin/view/LHCb/EventModelReview>
- [12] Private communication (Note in preparation)